

# ChemComm

Accepted Manuscript



This is an *Accepted Manuscript*, which has been through the Royal Society of Chemistry peer review process and has been accepted for publication.

*Accepted Manuscripts* are published online shortly after acceptance, before technical editing, formatting and proof reading. Using this free service, authors can make their results available to the community, in citable form, before we publish the edited article. We will replace this *Accepted Manuscript* with the edited and formatted *Advance Article* as soon as it is available.

You can find more information about *Accepted Manuscripts* in the [Information for Authors](#).

Please note that technical editing may introduce minor changes to the text and/or graphics, which may alter content. The journal's standard [Terms & Conditions](#) and the [Ethical guidelines](#) still apply. In no event shall the Royal Society of Chemistry be held responsible for any errors or omissions in this *Accepted Manuscript* or any consequences arising from the use of any information it contains.

## COMMUNICATION

# Surface chemistry and entrapment of magnesium nanoparticles into polymeric micelles: a highly biocompatible tool for photothermal therapy.

Cite this: DOI: 10.1039/x0xx00000x

Received 00th January 2012,  
Accepted 00th January 2012

E. Locatelli,<sup>a</sup> P. Matteini,<sup>b</sup> F. Sasdelli,<sup>c</sup> A. Pucci,<sup>a</sup> M. Chiariello,<sup>c</sup> V. Molinari,<sup>a</sup> R. Pini,<sup>b</sup> M. Comes Franchini.<sup>a,\*</sup>

DOI: 10.1039/x0xx00000x

[www.rsc.org/](http://www.rsc.org/)

**Abstract.** A novel highly biocompatible nanosystem containing Mg nanoparticles is reported, characterized and tested as suitable and non-toxic tool for photothermal therapy.

To date, the application of nanotechnology to healthcare, i.e. nanomedicine, raises enormous expectations in providing exhaustive answers to topical biomedical challenges.<sup>1</sup> However, despite the many advantages of nanomaterials, increasing concerns have been expressed on their potential adverse human health effects. Indeed, there exist several nanoscaled materials for human use on the market but only scarce knowledge on their health risks, safety data and toxicity profiles. For this reason, most of the scientific efforts are now addressed in investigating the toxicity and exposure pathways of those materials.<sup>2</sup> Up to now, several gold, iron, silver and metal oxides nanoparticles have been proposed for biomedical applications but it is matter of investigation by the Food and Drug Administration (FDA) to ensure development of both safe and efficacious nanoproducts.<sup>3</sup>

“Green nanotechnology” refers to the development of clean technologies, which should minimize the potential environmental and human health risks associated with the use of nanotechnology products, and encourage the replacement of existing products with new, less toxic, nanomaterials. The introduction of safer metals would certainly be an important point along this route. Recently, there has been increasing interest in magnesium as biomaterial.<sup>4</sup> There is about 20-30 grams of magnesium in the human body, of which 70% is in bone and teeth tissue. Magnesium is the fourth most abundant cation in the human body, and it is essential for human metabolism as well as for playing other important roles in the biological system. Overall, the safety of the magnesium nanoparticle lies in its biodegradation into magnesium ions, which are completely absorbable by the human body.

On the other hand, synthetic chemistry of magnesium nanoparticles is quite challenging because of its high reduction potential and very

high affinity toward oxidation. Magnesium nanoparticles have been prepared by different routes such as electrochemical reduction,<sup>5</sup> sonoelectrochemistry,<sup>6</sup> infiltration of nanoporous carbon with molten magnesium,<sup>7</sup> gas phase synthesis,<sup>8</sup> deposition from ethereal solutions,<sup>9</sup> high energy ball milling, and gas-condensation method.<sup>10</sup> Photothermal effects were ascribed to Mg NPs introduced into a biological sample and then irradiated with an IR laser.<sup>11</sup> Describing theoretical simulation and experimental measurements with unfunctionalized Mg NPs, the authors tested a direct injection of the NPs into the tissues and highlighted that there are still many problems to overcome before application in clinics. We believe that an easier handling and a clearer understanding of the surface chemistry of Mg NPs would be highly desirable for the fabrication of safer nanomaterials to be proposed for laser therapies. In this context, even if a small increase (4-5 °C) in tumor localized temperature has been demonstrated to sensitize cancer cells to concomitant radiation or chemotherapy, with little effects on normal cells,<sup>12</sup> therefore the obtainment of this aim with safe and efficient metals is still a challenge.

Herein, we report the synthesis of Mg NPs and their subsequent surface functionalization based on a simple ligand exchange, which provides suitability for entrapment into a polyethylene glycol (PEG)-based polymeric shell. Finally, the photothermal properties of these particles were tested and discussed on the basis of their *in vitro* toxicological response.

Due to the Mg high reduction potential and strong oxygen affinity, Mg NPs need to be synthesized under a constant flux of argon in order to avoid oxidation of the surface to magnesium oxide. We synthesized the Mg crystals in THF by reducing MgCl<sub>2</sub> with metallic lithium and exploiting naphthalene as electron carrier.<sup>12b</sup> After 20 minutes from lithium addition the reaction mixture turns from white to black with green shade, which is ascribed to the formation of a lithium-naphthalene complex, i.e. the real reducing agent. Reagents ratios were changed in order to better understand the reaction limits. In brief, keeping constant the MgCl<sub>2</sub> amount, lithium equivalents

(1.8, 2.5, 3.6) and naphthalene concentration (200, 150, 100, 50 or 20 mM) were varied. In this range, particles formation is not influenced by the lithium amount while the naphthalene concentration is an important parameter since no reaction was observed when the concentration was too low (under 100 mM), in all the other cases the reaction started after 20-30 minutes. Due to these preliminary observations, 3.6 equivalents of lithium and a 150 mM concentration of naphthalene were chosen for the Mg NPs synthesis. We noted that also the reaction time plays an important role because only after 24 hours Mg crystals are stable and can be recovered from the supernatant phase without aggregation phenomena. Conversely, if the reaction is stopped before this time, nanoparticles may form aggregates of more than 5  $\mu\text{m}$  in size. Dynamic light scattering (DLS) analysis showed a high hydrodynamic diameter of naked Mg particles ranging between 600 and 800 nm with polydispersity index (PDI) values ranging between 0.300 and 0.400 (**Figure S1**). Moreover, X-ray diffraction (XRD) measurements showed that particles are highly crystalline presenting the typical pattern of hexagonal magnesium in its reduced state (JCPDS no. 04-0770, **Figure S2**). In the diffractogram it is possible to discern two wide peaks in the background probably due to remaining  $\text{MgCl}_2$  or to an oxidized form of Mg. Energy-dispersive X-Ray spectroscopy analysis confirmed the presence of Mg as main element associated with  $\text{Cl}^-$  ions (**Figure S3**). Transition electron microscopy (TEM) showed that hexagonal platelets of Mg were formed during the reaction. The nanoparticles appear highly heterogeneous in size with an average diameter of about 50 nm and they are usually aggregated in sub-micron clusters due to the absence of any stabilizing agent (**Figure 1a and S4**).

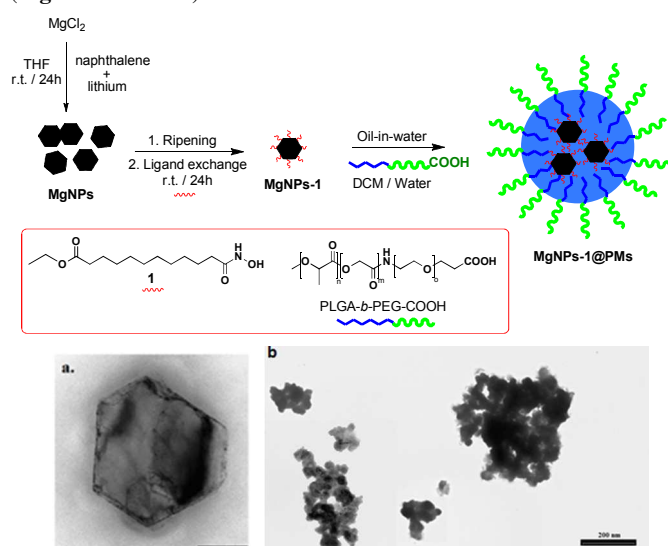


**Figure 1:** schematic pathway for the synthesis of MgNPs-1@PMs (above).

a) TEM image of MgNPs (scale bar 20 nm); b) TEM image of MgNPs-1@PMs (scale bar 200 nm);

In order to lower the degree of aggregation and to reduce and uniform the size, the nanocrystals were ripened with aliphatic amines: hexadecylamine, decylamine, octylamine and butylamine were investigated as ripening agents (**Table S1**). Upon incubation and following purification of MgNPs the DLS analysis revealed a decreasing trend of hydrodynamic diameter with the carbon-chain length of the used amine: the less the length the less the final

diameter. Butylamine, giving a diameter of  $322 \pm 3$  nm and a PDI value of  $0.290 \pm 0.006$ , was then selected as ripening agent. To improve the stability to air and water as well as their lipophilicity necessary for the following steps, the nanocrystals particles were coated with the ligand 12-ethoxy ester dodecanhydroxamic acid (**1**) synthesized as previously reported (**Figure 1**).<sup>13</sup>

The so-obtained MgNPs-1 are highly lipophilic and can be easily re-dispersed into organic solvent such as chloroform or dichloromethane. The hydrodynamic diameter resulted unchanged ( $311 \pm 1$  nm), suggesting a good stability of the hybrid structure (**Figure S5**). IR and thermo-gravimetric analysis (TGA) were carried out in order to confirm the ligand attachment. By comparing the IR spectra of Mg NPs, ligand **1**, and MgNPs-1 it is noticeable the presence of the ligand onto the nanoparticles surface (**Figure S6**) while TGA revealed that the ligand on the surface of the nanoparticles accounted for 26% of the total weight (**Figure S7**). Moreover, inductively coupled plasma emission spectrometry (ICP) measurements showed a high concentration of magnesium in the solution (0.747 mg/mL, 31.1 mM).

The hydrophobic nanoparticles were then entrapped into water-dispersible polymeric micelles (PMs) using the oil-in-water emulsion solvent technique (**Figure 1**);<sup>14</sup> particularly the FDA-approved targetable PLGA-*b*-PEG-COOH copolymer<sup>15</sup> was used for the entrapment of the MgNPs-1: the so-obtained MgNPs-1@PMs were purified and fully characterized. DLS analysis (**Figure 1**) showed a hydrodynamic diameter of  $319 \pm 10$  nm and a narrow size distribution (PDI =  $0.24 \pm 0.01$ ). As expected, due to the presence of carboxylic acid groups in the micelles outer shell, the  $\zeta$ -potential value is negative (-26.1 mV) suggesting nanoparticles stabilization and suitability for *in-vivo* experiments.<sup>16</sup> TEM (**Figure 1b and S8**) and STEM (**Figure S8**) observations confirmed these results showing magnesium nanoparticles surrounded by a polymeric matrix with diameter comparable to those obtained by DLS. As predictable by the grayish color of the micelle dispersion, XRD analysis (**Figure S9**) demonstrated that the Mg NPs mainly maintained their electronic state throughout the process. The formation of a thin layer of brucite (JCPDS no. 83-0114) was detected which probably helped in passivating the nanostructures. The XRD measurements on MgNPs-1@PMs were repeated after 5 and 20 days from the synthesis. The nanoproduct displayed no changes within this time range excluding the occurrence of any further oxidation process. ICP analysis showed a Mg amount of 0.130 mg/mL meaning that a high concentration (5.4 mM) of magnesium into the final nanocarrier was achieved.

The optical analysis of the final MgNPs-1@PMs revealed an extinction signal covering the whole visible spectrum and extending toward the near infrared (NIR) region (**Figure S10**). This suggest the possibility of using a NIR laser illumination in order to obtain a photothermal response from MgNPs-1@PMs. Worth noting is that NIR light is highly preferable with a view to biomedical applications due to its higher penetration inside human tissues.<sup>17</sup> Thus, we proved the possibility of generating a temperature rise of a few to several degrees once nanoparticles batches containing 5.3 mM of Mg were illuminated with a 810 nm diode laser operated in continuous wave (cw) mode. The temperature can be regulated by varying the laser intensity (namely, power per surface unit) and with a linear dependence within the 5-31  $\text{W cm}^{-2}$  range (**Figures 2a**). The observed linearity suggests effective stability of the particles against

thermal modifications within a temperature gradient of interest for local hyperthermia.<sup>18</sup> The photothermal conversion is estimated of ~80% originated by the reduced Mg content of MgNPs-1@PMs and the remaining by the polymeric shell enwrapping the particle core (Figure S11). Finally, we investigated whether the photothermal response could vary as a function of Mg concentration. This is of relevance for the biomedical application of MgNPs-1@PMs where a dilution of the initial particles batch (i.e. upon introduction in cell cultures or in the human body) is expected. A plot of the maximum temperature gradients registered against different concentration values of Mg is reported in Figure 2b. The results suggest that an effective photothermal response can be obtained down to submillimolar concentration values of Mg, corresponding to few tens of mg/L of nanoparticles, which are typically contemplated within the protocols of photothermal therapies.<sup>19</sup>

Although magnesium can be considered a safe biomaterial, we set-up to investigate potential cytotoxicity of the fully assembled magnesium-loaded nanoparticles. As a model system, we used HN13 epithelial cells, derived from a head and neck squamous cell carcinoma.<sup>20</sup> To this aim, we decided to focus our attention on MgNPs-1@PMs concentrations that could grant us a  $\Delta T_{\text{max}}$  potentially useful for future applications as adjuvant photothermal therapy.

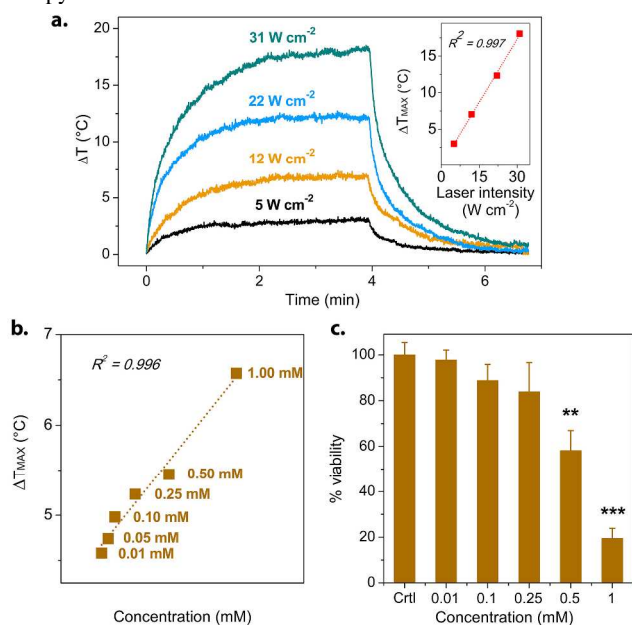


**Figure 2:** a) temperature profiles obtained by illuminating MgNPs-1@PMs (5.3 mM of Mg) with increasing laser intensities at a fixed  $t_{\text{irr}} = 4$  min and diagram of  $\Delta T_{\text{max}}$  increase from (a) vs. laser intensity. b)  $\Delta T_{\text{max}}$  increase versus Mg concentration obtained with a  $22 \text{ W cm}^{-2}$  laser intensity. c) toxicity evaluation of MgNPs-1@PMs at different concentrations, obtained by Trypan blue exclusion assay. The results shown are averages  $\pm$  SEM of triplicate samples from a typical experiment. Measures were subjected to one-way ANOVA test.  $p < 0.01$  (\*\*),  $p < 0.001$  (\*\*\*)

Very low toxicity was observed for nanoparticles containing up to  $250 \mu\text{M}$  in Mg (Figure 2c), a value corresponding to a significant  $\Delta T_{\text{max}}$  of  $\sim 5 \text{ }^\circ\text{C}$  (Figure 2c), when the particles are illuminated with a  $22 \text{ W cm}^{-2}$  laser intensity. We may note that similar laser parameters have been previously used in a number of minimally

invasive laser therapies based on the combined use of NIR light and organic or metal nanochromophores.<sup>21</sup> These results, therefore, suggest that magnesium nanoparticles can be safely used for medical applications dealing with laser-induced heating.

## Conclusions

In summary, we have developed a phase transfer process to obtain lipophilic Mg NPs by a reproducible ligand exchange with subsequent entrapment of the particles into PEG-based micelles. The utility of this approach arises from the possibility to manipulate the Mg NPs in organic solvent and to build PEG-based targetable nanostructures that are non-toxic within a concentration range useful for biomedical applications. Finally, we proved that the MgNPs-1@PMs can be excited with a cw NIR laser light to produce localized temperature gradients of at least  $4\text{--}5 \text{ }^\circ\text{C}$ . Despite the lower photothermal efficiency of Mg with respect to Au NPs, we consider MgNPs as a promising candidate for future minimally invasive laser therapies with the potential to replace the metal NPs conventionally used, at least when an heating in the range of hyperthermia treatments is required.

## Notes and references

- <sup>a</sup> Department of Industrial Chemistry "Toso Montanari". University of Bologna. Viale Risorgimento 4, 40136 Bologna (Italia). Fax: 051-2093654. Phone: 051-2093626. Email: mauro.comesfranchini@unibo.it
- <sup>b</sup> Institute of Applied Physics "Nello Carrara", National Research Council. Via Madonna del Piano 10, 50019 Sesto Fiorentino (Italy)
- <sup>c</sup> Istituto Toscano Tumori, Core Research Laboratory and Istituto di Fisiologia Clinica, Consiglio Nazionale delle Ricerche, Siena, Italy
- <sup>†</sup> Electronic Supplementary Information (ESI) available: See DOI: 10.1039/c000000x/
- <sup>1</sup> S. C. Kumar (ed) in *Nanomaterials for Medical Diagnosis and Therapy and Nanomaterials for Cancer Therapy*, Nanotechnologies for the life sciences, Vol. 10 and Vol. 6, Wiley-VCH, Weinheim, Germany 2007.
- <sup>2</sup> A. Tajani, *Nat. Nanotechnol.*, 2013, **8**, 306.
- <sup>3</sup> a) N. Sanvincens, M. P. Marco, *Trends in Biotechnol.*, 2008, **26**, 425. b) R. Gaspar, *Nanomed.*, 2007, **2**, 143.
- <sup>4</sup> a) J. Walker, S. Shadanbaz, T. B. F. Woodfield, M. P. Staiger, G. J. Dias, *J. Biomed. Mater. Res. Part. B*, 2014, DOI: 10.1002/jbm.b.33113. b) C. Jin, Z. Z He, J. Zhang, X. Y. Yang, J. Liu, *J. Nanotechnol. Eng. Med.*, 2013, **4**(1), 11004.
- <sup>5</sup> K. F. Aguey-Zinsou, J. R. Ares-Fernandez, *Chem. Mater.*, 2008, **20**, 376.
- <sup>6</sup> I. Haas, A. Gedanken, *Chem. Commun.*, 2008, 1795.
- <sup>7</sup> P. E. de Jongh, R. W. P. Wagemans, T. M. Eggenhuisen, B. S. Dauvillier, P. B. Radstake, J. D. Meeldijk, J. W. Geus, K. P. de Jong, *Chem. Mater.*, 2007, **19**, 6052.
- <sup>8</sup> B. J. Kooi, G. Palasantzas, J. T. M. de Hosson, *Appl. Phys. Lett.*, 2006, **89**, 161914.
- <sup>9</sup> D. Aurbach, Z. Lu, A. Schechter, Y. Gofer, H. Gizbar, R. Turgeman, Y. Cohen, M. Moshkovich, E. Levi, *Nature*, 2000, **407**, 724.
- <sup>10</sup> H. R. Peng, L. C. Zhu, Z. K. Zhang, *Compos. Interfaces*, 2004, **112**, 231.
- <sup>11</sup> Q. Wang, L. Xie, Z. He, D. Di, J. Liu, *Int. J. Nanomed.*, 2012, **7**, 4715.

- <sup>12</sup> a) D. K. Chatterjee, P. Diagaradjane, S. Krishnan, *Ther. Deliv.*, 2011, **2**, 1001. b) M. R. Song, M. Chen, Z. J. Zhang, *Mater. Charact.*, 2008, **59**, 514.
- <sup>13</sup> a) M. Comes Franchini, G. Baldi, D. Bonacchi, D. Gentili, G. Giudetti, A. Lascialfari, M. Corti, P. Marmorato, J. Ponti, E. Micotti, U. Guerrini, L. Sironi, P. Gelosa, C. Ravagli, A. Ricci, *Small*, 2010, **6**(3), 366. b) G. Baldi, D. Bonacchi, M. Comes Franchini, D. Gentili, G. Lorenzi, A. Ricci, C. Ravagli, *Langmuir*, 2007, **23**(7), 4026.
- <sup>14</sup> J. Kreuter, *Encycl Nanosci Nanotechnol*, 2004, **7**, 161.
- <sup>15</sup> E. Locatelli, M. Comes Franchini, *J. Nanopart. Res.*, 2012, **14**, 1316.
- <sup>16</sup> S. Honary, F. Zahir, *Tro. J. Pharma. Res.*, 2013, **12**, 255.
- <sup>17</sup> K. Welsher, Z. Liu, S. P. Sherlock, J. T. Robinson, Z. Chen, D. Daranciang, H. Dai, *Nat. Nanotechnol.*, 2009, **4**, 773.
- <sup>18</sup> a) G. von Maltzahn, J. H. Park, A. Agrawal, N. K. Bandaru, S. K. Das, M. J. Sailor, S. N. Bhatia, *Cancer Res.*, 2009, **69**, 3892. b) P. Matteini, F. Ratto, F. Rossi, R. J. Pini, *J. Biomed. Opt.*, 2012, **17**, 0107011. c) P. Matteini, F. Tatini, L. Luconi, F. Ratto, F. Rossi, G. Giambastiani, R. Pini, *Angew. Chem. Int. Ed.*, 2013, **52**, 5956. d) P. Matteini, M. R. Martina, G. Giambastiani, F. Tatini, R. Cascella, F. Ratto, C. Cecchi, G. Caminati, L. Dei, R. Pini, *J. Mater. Chem. B*, 2013, **1**, 1096.
- <sup>19</sup> a) P. Matteini, F. Ratto, F. Rossi, S. Centi, L. Dei, R. Pini, *Adv. Mater.*, 2010, **22**, 4313. b) T. J. Robinson, S. M. Tabakman, Y. Liang, H. Wang, H. S. Casalongue, D. Vinh, H. Dai, *J. Am. Chem. Soc.*, 2011, **133**, 6825.
- <sup>20</sup> V. Sriuranpong, J. I. Park, P. Amornphimoltham, V. Patel, B. D. Nelkin, J. S. Gutkind, *Cancer Res.*, 2003, **63**, 2948.
- <sup>21</sup> a) P. Matteini, F. Ratto, F. Rossi, F. M. de Angelis, L. Cavigli, R. Pini, *J. Biophotonics*, 2012, **5**, 868. b) P. Matteini, F. Ratto, F. Rossi, G. Rossi, G. Esposito, A. Puca, A. Albanese, G. Maira, R. Pini, *J. Biomed. Opt.*, 2010, **15**, 041508. c) G. Esposito, F. Rossi, P. Matteini, A. Scerrati, A. Puca, A. Albanese, G. Rossi, F. Ratto, G. Maira, R. Pini, *Lasers Surg. Med.*, 2013, **45**, 318.